THE ASTROPHYSICAL JOURNAL, 211:135–146, 1977 January 1

THE EVAPORATION OF SPHERICAL CLOUDS IN A HOT GAS. I. CLASSICAL AND SATURATED MASS LOSS RATES

LENNOX L. COWIE
Physics Department, Harvard University
AND
CHRISTOPHER F. MCKEE
Physics Department and Astronomy Department, University of California, Berkeley
Received 1976 April 30; revised 1976 June 25

ABSTRACT

In this and two subsequent papers we develop analytic solutions for the rate of evaporative mass loss from an isolated spherical cloud embedded in a hot tenuous gas. In the present paper we consider systems in which the effects of radiation and magnetic fields may be neglected; these effects will be considered in the two subsequent papers. It is pointed out that in many cases of interest the classical form of the thermal conduction is inapplicable and an upper bound to the heat flux which may be carried by the electrons is derived which is substantially lower than most previous estimates. Eigenvalues of the time-independent energy conservation equations are found both in the case where the classical conduction is applicable throughout the interface and in the case where the heat flux reaches its limiting value. (We refer to this as saturation.) The dynamics of the flow from the cloud is analyzed in both cases, and the use of the time-independent equations is justified. The theory is compared with the theory of thermal conduction fronts described by McKee and Cowie. Finally we consider the application of the theory to clouds within supernova remnants where anisotropy and dynamical effects are important. Discussion of the applications of these results is deferred to Paper II, where the effects of radiation are considered.

Subject headings: interstellar: matter — nebulae: general — nebulae: supernova remnants

I. INTRODUCTION

Thermal conduction processes, while extensively considered in the case of the solar wind and corona, have seldom been thought to be of much importance in other astrophysical systems, and in particular to have little effect on the dynamics or thermal balance of the interstellar gas. Some exceptions to this must be noted, however, and the effects of electron thermal conduction on the energy balance of a galactic corona (Spitzer 1956) and on the stabilization of radiatively cooling gas (Field 1965) have been considered in some detail. More recently the importance of conduction in the evolution of supernova remnants (Chevalier 1975*a*, *b*; Solinger, Rappaport, and Buff 1975) and on the evolution of gas within clusters of galaxies (Lea 1974) has been pointed out.

Neglect of thermal conduction in the interstellar gas was justified by the comparatively low temperatures ($\lesssim 10^4$ K) and high densities ($\gtrsim 0.3$ cm^{-3}) considered characteristic of the interstellar gas (e.g., Spitzer 1968). Only recently has evidence from the O VI absorption lines detected by *Copernicus* (Jenkins and Meloy 1974) and from the uniform soft X-ray background (Williamson *et al.* 1974) indicated the presence of a higher temperature ($\sim 10^6$ K, $n \sim 10^{-2}$ cm^{-3}) component of the gas. Whatever the theoretical interpretation of this gas (Castor, McCray, and Weaver 1975; Cox and Smith 1974; McKee and Ostriker 1975), it is clear that thermal conduction processes will play a dominant role in its evolution, since the conductive heat flux in a fully ionized plasma is an extremely sensitive function of temperature ($\propto T^{7/2}$, Spitzer 1962).

Finally, in addition to the problems mentioned above, thermal conduction should play an important (and as yet unconsidered) role in the evolution of gas in elliptical galaxies and in the evolution of intergalactic medium gas. Of particular interest is the interaction of intergalactic or intracluster hot gas with the gas within galaxies (De Young 1973).

One of the most important effects of thermal conduction is the evaporation of density inhomogeneities or "clouds," and this is the topic we shall consider here. While particular solutions to this problem exist (Zel'dovich and Pikel'ner 1969; Penston and Brown 1969; Graham and Langer 1973; Chevalier 1975*b*), most emphasizing the case of interstellar clouds evaporating in an intercloud medium ($T \sim 10^4$ K, $n \sim 0.3$ cm^{-3}), no attempts at a general solution have as yet been made. In particular most of the solutions have been numerical, and it is difficult to scale the results to conditions of different ambient temperature and density. In this paper (Paper I) and in two subsequent papers (McKee and Cowie 1977*a*, *b* [Papers II and III]), we shall obtain analytic solutions for the case of a spherical cloud embedded in a hot tenuous gas.

In Paper II we shall discuss the conditions under

which radiative losses play an important role in the evaporative process, and obtain solutions for the radiative losses in the evaporating interface, while in Paper III we shall consider the importance of the magnetic field configurations in determining the rate of evaporative mass loss. There we shall show that under a wide variety of conditions the presence of a magnetic field does not significantly affect the evaporation. In the present paper (Paper I) we shall obtain analytic solutions for the cases in which radiation and magnetic fields may be ignored. We consider only the evaporation of spherical clouds where the evaporative mass loss rate is an eigenvalue of the time-independent energy conservation equation. As we shall discuss, these solutions may normally be expected to be accurate approximations to the exact time-dependent mass loss rates. Such solutions are, however, unique to the spherical geometry, and different (time dependent) methods are required for the evaporation of plane and cylindrical clouds.

In those cases where the classical thermal conduction formula (e.g., Spitzer 1962) is applicable throughout the interface, the solution for the evaporation rate is straightforward and is described in § III. Unfortunately, for many situations of interest, the mean free path of the electrons in the hot gas is not small compared with the radius of the evaporating cloud. In such cases we may no longer use the classical theory of thermal conduction, which is based on a diffusion approximation (Parker 1963). (We may note that when the classical theory is incorrectly applied to systems in which the approximation has broken down, it can result in gross overestimates of the importance of thermal conduction). In § II we consider the upper bound on the heat flux which may be carried by the electrons, and conclude that this is smaller than has previously been considered. For collisionless gases the exact heat flux should closely approximate this maximum value, and indeed, as we shall discuss in § II*b*, the theory gives good numerical agreement with solar wind observations.

Derivation of the evaporative mass loss rate when the classical conduction formula is not applicable throughout the interface is substantially more complicated than in the classical case. However, it is still possible to obtain analytic solutions under certain limitations, and these are given in § IV. Readers primarily interested in the results may wish to omit the analysis in §§ IV*a*–IV*e* and note only the mass loss rate given in equation (68). The restrictions of the model are considered in § IV*f*, where it is shown that the theory is adequate for most cases of interest.

In § V we compare the results of our present theory with a previous, less accurate analysis in terms of conduction fronts, which are analogous to ionization fronts (McKee and Cowie 1975). The conduction front, or thermal wave (Zel'dovich and Raizer 1966), moving into the cloud is usually D-type.

The theory of §§ III and IV is premised on an isolated spherical cloud in which departures from spherical symmetry are neglected. The theory as such is not directly applicable to a number of systems of interest, most particularly the evaporation of clouds within supernova remnants (McKee and Cowie 1975; Chevalier 1975*b*). In § VI we discuss the evaporation of clouds in such systems and conclude that even in such an extreme case the results of §§ III and IV should provide a reasonable approximation.

Finally in § VII we summarize the results, postponing discussion of the applications to the final section of Paper II, where the effects of radiation are also included.

II. SATURATED THERMAL CONDUCTION

a) Classical and Saturated Heat Fluxes

The thermal conductivity in a fully ionized hydrogen plasma, in which many collisions take place over the scale length for temperature variation, is given by (Spitzer 1962)

$$\kappa = \frac{1.84 \times 10^{-5} T_e^{5/2}}{\ln \Lambda} \text{ ergs s}^{-1} \text{ deg}^{-1} \text{ cm}^{-1}, \quad (1)$$

where for $T > 4.2 \times 10^5$ K the Coulomb logarithm is

$$\ln \Lambda = 29.7 + \ln n^{-1/2} (T_e / 10^6 \text{ K}). \quad (2)$$

The heat is conducted by the electrons, and equation (1) includes the effect of the self-consistent electric field required to maintain the electric current at zero; this reduces κ by a factor of about 0.4 from the value it would otherwise have.

The conductivity is directly proportional to the mean free path λ for electron energy exchange:

$$\lambda = t_{\rm eq} \left(\frac{3kT_e}{m_e} \right)^{1/2}, \quad (3)$$

where $t_{\rm eq}$, the electron-electron equipartition time, is (Spitzer 1962)

$$t_{\rm eq} = \frac{3 m_e^{1/2} (kT_e)^{3/2}}{4\pi^{1/2} n_e e^4 \ln \Lambda}. \quad (4)$$

Here n_e is the electron density, and the other symbols have their usual meaning. The equipartition time is only slightly larger than the time in which collisions with other electrons cause the trajectory of a typical electron to be deflected by 90°. The equivalent mean free path for ions has approximately the same value, since λ is independent of m_e; numerically $\lambda \approx 10^4 T^2/n$ cm. In terms of λ, the thermal conductivity is

$$\kappa = 1.31 n_e k \lambda (kT_e/m_e)^{1/2}; \quad (5)$$

and the heat flux

$$q = -\kappa \nabla T \quad (6)$$

is proportional to λ/L_T, where L_T is the temperature scale height $T/|\nabla T|$.

The classical thermal conductivity (eq. [1]) is based on the assumption that the mean free path is short ($\lambda \ll L_T$). When the mean free path becomes comparable to or even greater than the temperature scale

height, the heat flux is no longer equal to $-\kappa\nabla T$: we describe this effect as *saturation*. The maximum heat flux in a plasma can be expressed as $(3/2)n_e k T_e v_{\rm char}$, where $v_{\rm char}$ is a characteristic velocity which one might expect to be of the order of the electron thermal velocity (Parker 1963). However, by a suitable choice of distribution function, it is possible to make $v_{\rm char}$ arbitrarily large (Manheimer and Klein 1975).

The actual magnitude of the "saturated" flux is determined by the nature of the heat source and by two constraints on the electron distribution function: first, that it carry no current, since otherwise large electrostatic fields would build up,[1] and second, that it be stable against the various plasma instabilities which tend to drive an anisotropic distribution toward isotropy. Parker's (1963) estimate of $v_{\rm char} = (3kT_e/m_e)^{1/2}$ corresponds to the electrons streaming past the ions at the thermal velocity; as such it violates the zero current requirement and is also unstable against the ion acoustic instability (Forslund 1970).

Morse and Nielsen (1973) have discussed the saturation problem in the context of laser-heated plasmas. They considered a one-dimensional distribution function, $f(v)$, consisting of two components: "hot" particles with $0 \leq v \leq v_{\rm hot}$ and $f(v) = n_{\rm hot}/v_{\rm hot}$, and backward moving "cold" particles with $-v_{\rm cold} \leq v \leq 0$ and $f(v) = n_{\rm cold}/v_{\rm cold}$. Fixing $v_{\rm hot}$ and imposing the zero current requirement, they found that the maximum possible heat flux was $(1/32)nmv_{\rm hot}^3$. In three dimensions the same result holds, corresponding to $v_{\rm char} = 0.66(kT/m_e)^{1/2}$, where T is the average temperature of both the hot and the cold particles. They supported their estimate by numerical simulations; however, simulations by Manheimer and Klein (1975), in which the system was allowed to relax to a steady state, give a value several times smaller. Although Morse and Nielsen's distribution function is stable against electrostatic streaming instabilities, it is possible that it is unstable against instabilities of the Weibel (1959) type.

We are interested in the case in which the heat source (e.g., the Sun, or a hot gas surrounding a cloud) has a Maxwellian distribution. An approximate upper limit to the saturated heat flux in this case is the heat flux due to a Maxwellian distribution in the presence of an infinite temperature gradient—a hot gas abutting a cold absorber. In the absence of the zero current requirement, this would be the free molecular conductivity (cf. Williams 1971) obtained by averaging $\frac{1}{2}v^3 \cos\theta$ over $0 \leqslant \theta \leqslant \pi/2$, where $\theta = 0$ is the direction of the heat flux; the result is $v_{\rm char} = (8/9\pi)^{1/2}(kT/m_e)^{1/2}$. Just as in the classical case, however, a self-consistent electric field will be set up to stop the current. We assume that the heat flux is reduced by the same factor of 0.4 in the saturated case as in the classical case so that the saturated heat flux is

$$q_{\rm sat} = 0.4\left(\frac{2kT_e}{\pi m_e}\right)^{1/2} n_e k T_e \,. \tag{7}$$

[1] More precisely, the divergence of the current density must vanish; for spherical symmetry this reduces to the condition above.

This result for $q_{\rm sat}$ does not depend sensitively on the distribution function; had we chosen a uniform distribution function ($f[v] = $ const.) instead of a Maxwellian, $q_{\rm sat}$ would have been reduced by only about 10%. The estimate for the maximum steady heat flux in a plasma given by equation (7) is 8.1 times less than Parker's (1963) estimate and 3.1 times less than Morse and Nielsen's (1973) estimate, but it is comparable to Manheimer and Klein's (1975) estimate. The validity of our estimate must be determined by comparison with observation (see below) and by future theoretical work. As we shall see later, the fact that the saturated heat flux is significantly less than conjectured by Parker (1963) implies that the evaporative flow is not highly supersonic and allows us to integrate the equation of motion and the energy equation separately.

In order to explicitly allow for the uncertainty in our estimate of $q_{\rm sat}$, we introduce a factor ϕ_s which is of order unity and rewrite equation (7) as

$$q_{\rm sat} = 5\phi_s \rho c^3 = 5\phi_s c p \,, \tag{8}$$

where $c^2 = p/\rho$ is the isothermal sound speed, p is the pressure, and ρ is the density. If the saturated heat flux $q_{\rm sat}$ is correctly given by equation (7) and if the electron and ion temperatures are equal, then $\phi_s = 1.1$ for a fully ionized gas with cosmic abundances. For $T_e \neq T_i$, equation (7) is unaffected; but the factor $[2T_e/(T_e + T_i)]^{3/2}$ must be included in ϕ_s in equation (8).

Both plasma turbulence and magnetic fields can reduce $q_{\rm sat}$. When the heat flux is saturated, the collisional mean free path λ is large ($\lambda \gtrsim L_T$) and some plasma turbulence can be expected in order to maintain approximate isotropy of the electrons. To some extent, the effects of this level of turbulence have already been included, since our estimate of $q_{\rm sat}$ is based on the assumption that the electrons are nearly isotropic. Higher levels of plasma turbulence which reduce the effective mean free path significantly below the temperature scale length L_T will correspondingly reduce ϕ_s. As we shall see shortly, the level of plasma turbulence in the quiet solar wind does not reduce $q_{\rm sat}$ below our estimate.

The above expressions for both the classical and saturated heat fluxes apply only in the direction parallel to any magnetic field which may be present; the conduction perpendicular to the magnetic field is determined by the gyroradius of the particles and is negligible for most astrophysical problems. When a uniform magnetic field lies at an angle θ to the direction of the temperature gradient, the classical heat flux parallel to the gradient is reduced by a factor of $\cos^2\theta$. The first factor of $\cos\theta$ corresponds to the projection of the temperature gradient onto the magnetic field and the second factor arises from the projection of the resulting heat flux which is parallel to the field back onto the direction of the gradient. However, since the saturated heat flux is independent of ∇T, it is reduced by only the second factor of $\cos\theta$. This factor enters into ϕ_s and reduces its value. We shall discuss the role of magnetic fields in detail in Paper III (McKee and Cowie 1977*b*).

An important parameter in our analysis is the ratio of the classical heat flux to the saturated heat flux, which we denote by σ. In terms of the temperature scale height L_T defined above we have

$$\sigma = \frac{\kappa T_e}{5\phi_s \rho c^3 L_T} \tag{9}$$

$$= \frac{4.6\lambda}{\phi_s L_T}, \tag{10}$$

where we have used equation (5) in the last step and inserted numerical values appropriate for $T_e = T_i$ and a helium abundance of 10% by number. The transition from classical ($\sigma \ll 1$) to saturated ($\sigma \gg 1$) heat flow occurs at $\sigma \sim 1$. Since this corresponds to $\lambda \sim 0.2\phi_s L_T$, the gas is still collision dominated at the onset of saturation.

b) *Comparison with the Solar Wind*

Thermal conduction plays an important role in providing energy to the solar wind (Parker 1963), but uncertainty concerning the transport coefficients in dilute plasmas ($\lambda \sim L_T$) has prevented a satisfactory theoretical explanation of its effects in the solar wind. Observations show that the heat flux is less than that predicted from classical theory (Montgomery 1972*a*; Feldman *et al.* 1973), and models based on classical conduction give electron temperatures higher than observed (e.g., Cuperman and Metzler 1973).

Forslund (1970) suggested that plasma instabilities reduce the conductivity below the classical value. Perkins (1973) has shown that because most solar wind electrons bounce between the Sun and an electrostatic potential barrier, the conductivity is reduced; however, he argues that plasma instabilities per se do not reduce the conductivity. Hollweg (1974) pointed out that the electrons which are not in bound orbits provide a collisionless (i.e., saturated) heat flux which can be much larger than the collisional heat flux estimated by Perkins. Hollweg went on to suggest that plasma instabilities determine the magnitude of the saturated heat flux, but his first estimate of 1.45×10^{-3} ergs cm^{-2} s^{-1} is several times less than the observed value.

In the model of § II*a*, the principal effect of instabilities on solar wind electrons is to produce the observed isotropy, while the heat flux along the magnetic field is approximately given by $q_{\rm sat}$ in equation (7). Averaging of the *Vela-4* data gives $n_e = 7$ cm^{-3}, $T_e = 1.4 \times 10^5$ K, and a heat flux of 7×10^{-3} ergs cm^{-2} s^{-1} (Montgomery 1972*b*); equation (7) gives 6.3×10^{-3} ergs cm^{-2} s^{-1}. For the quiet solar wind ($v < 350$ km s^{-1}) the averages are $n_e = 8.3$ cm^{-3}, $T_e = 1.3\ 10^5$ K and a heat flux of 5×10^{-3} ergs cm^{-2} s^{-1}; in this case equation (7) yields 6.7×10^{-3} ergs cm^{-2} s^{-1}. The most direct evidence for saturation of the heat conduction has been presented by Feldman *et al.* (1973), who showed that $q/nT^{3/2}$ remained nearly constant for values of T ranging over a factor of 2. We conclude that our model of saturated thermal conduction is consistent with observations of the solar wind.

Within the context of a one-fluid model Cuperman and Metzler (1973) have shown that the observed properties of the solar wind are reproduced if the classical conductivity is reduced by the empirical factor $(r/R_\odot)^{-0.22} \cos^2 \psi(r)$, where $\psi(r)$ is the angle between the radial direction and the magnetic field. Utilizing the temperature and density profiles calculated by Cuperman and Metzler, we find that the ratio of saturated to classical heat fluxes agrees closely with the empirical reduction factor for all radii greater than a few solar radii. However, a full two-fluid calculation utilizing a saturated conductivity is clearly desirable.

In view of the complexity of the solar wind, our model is by no means a complete description. However, the numerical agreement between our model and these detailed observations encourages us to believe that it should provide a good approximation to other physical systems.

III. CLASSICAL EVAPORATION

a) *Evaporation Rates*

Throughout §§ III and IV we shall consider the evaporation of a spherical cloud of radius R embedded in a hot gas which has density n_f and temperature T_f far from the cloud, under the assumption that radiation, ionization, and magnetic fields may be neglected. (Ionization may be neglected if the surface of the cloud is ionized or if the ambient plasma is very hot, $kT_f \gg 1$ Ryd.) We seek time-independent solutions for the mass loss rate

$$\dot{m} = 4\pi r^2 \rho v \tag{11}$$

which are eigenvalues of the energy conservation equation

$$\nabla \cdot \rho v(\tfrac{1}{2}v^2 + 5c^2/2) + \nabla \cdot \boldsymbol{q} = 0 \tag{12}$$

subject to the boundary condition that T approaches T_f as r approaches infinity and $T \sim 0$ at $r = R$. Such solutions may be found only for spherical geometries, and the solutions described are not directly applicable to plane or cylindrical cases. (Time-independent solutions for the latter two cases exist only if T is constrained to approach T_f at a finite distance from the cloud.) For simplicity of notation we define the dimensionless variables

$$y = r/R, \tag{13}$$

$$\tau = T/T_f, \tag{14}$$

and

$$w = \dot{m}/\dot{m}_{\rm class}, \tag{15}$$

where

$$\dot{m}_{\rm class} = 16\pi\mu\kappa_f R/25k. \tag{16}$$

Here μ is the mean mass per particle so that $c^2 = kT/\mu$,

and κ_f is the value of the conductivity at temperature T_f.

In this section we shall derive a solution to equation (12) when the classical conduction formula is applicable throughout the interface between the cloud and the hot gas. The solution in this case is particularly simple since for small values of the quantity $\frac{1}{5}M^2$ (where M is the Mach number $= v/c$) the equations of motion and energy conservation are separable. As we shall show in § III*b*, this approximation is always satisfied.

Integration of the energy conservation equation (12) gives the equation

$$(5/2)\dot{m}gc^2 - 4\pi r^2\kappa \frac{dT}{dr} = A\,, \tag{17}$$

where A is the constant of integration, and

$$g = 1 + \tfrac{1}{5}M^2\,. \tag{18}$$

The integration constant A represents the difference between the outward enthalpy flux and the inward conductive heat flux; we assume that the cloud is cold relative to its surroundings so that both fluxes are negligible at the cloud surface and $A \approx 0$. One can show that this argument is valid even if the cloud itself is not ionized.

In terms of our dimensionless variables, equation (17) may be rewritten as

$$\tau^{3/2}\frac{d\tau}{dy} = \frac{2}{5}gw/y^2 \tag{19}$$

which is subject to the boundary conditions $\tau \simeq 0$ as $y \to 1$ and $\tau \to 1$ as $y \to \infty$. Our approximation consists of treating g as constant in the integration. Since this procedure is valid only for g of order unity, we shall in fact set $g = 1$ after integration. The eigenvalue of the equation is $w = 1/g \approx 1$, and the solution of equation (19) is

$$\tau = (1 - y^{-1})^{2/5}\,. \tag{20}$$

The mass loss rate from the cloud is then

$$\dot{m} = 16\pi\mu\kappa_f R/25k$$
$$= 2.75 \times 10^4 T_f^{5/2} R_{\rm pc}(30/\ln\Lambda)\ {\rm g\ s^{-1}}\,, \tag{21}$$

where $R_{\rm pc}$ is in parsecs, the Coulomb logarithm $\ln\Lambda$ is evaluated at $T = T_f$ and $n = n_f$, and we have set $g = 1$. The cloud will evaporate in a characteristic time

$$t_{\rm evap} = m_c/\dot{m} = 3.3 \times 10^{20}\bar{n}_c R_{\rm pc}{}^2 T_f{}^{-5/2}\frac{\ln\Lambda}{30}\ {\rm yr}\,, \tag{22}$$

where m_c and $\bar{n}_c$ are the mass and mean hydrogen density of the cloud, respectively. The numerical value assumes a 10% admixture of helium by number.

b) Dynamics

We have been able to integrate the energy equation (12) independently of the equation of motion under the assumption that the Mach number M is not large. This approximation is in fact equivalent to the assumption that the classical conductivity is applicable throughout the flow. From equation (12) we find that the ratio σ of the classical heat flux to the saturated heat flux $q_{\rm sat}$ is

$$\sigma = Mg/2\phi_s \tag{23}$$

provided $\sigma \lesssim 1$ so that the heat flux is not saturated. The Mach number at which $\sigma = 1$ and saturation occurs is $2\phi_s/g$, which is of order unity since ϕ_s is. Hence M is not large in classical evaporative flow.

With the temperature determined from the energy equation, analysis of the dynamics of the evaporative flow is straightforward. The time-independent equation of motion,

$$\rho v\frac{dv}{dr} = -\frac{dp}{dr}\,, \tag{24}$$

may be rewritten in the forms

$$\frac{d}{dr}(\ln v) = (1 - M^2)^{-1}\frac{d}{dr}(\ln T/r^2) \tag{25}$$

or

$$\frac{d}{dr}(\ln p) = -\frac{M^2}{1 - M^2}\frac{d}{dr}(\ln T/r^2)\,. \tag{26}$$

Furthermore, the heat flux q varies as T/r^2 according to equation (20). Hence for subsonic flow the maximum velocity, the minimum pressure and the maximum inward heat flux all occur at the maximum value of T/r^2 or, from equation (20), at $y = 1.2$. For transonic flow this is the sonic point where $M^2 = 1$.

Equation (25) may be combined with equation (20) to cast the equation of motion in the dimensionless form,

$$(1 - M^2)\frac{d\ln M^2}{dy}$$
$$= 0.4[2(6 - 5y) + M^2 - 1]/y(y - 1)\,. \tag{27}$$

The solutions curves of equation (27) are shown in (M^2, y)-space in Figure 1. These curves are not valid at Mach numbers much greater than 1, since our approximation that $g = 1 + M^2/5$ is constant breaks down and the shock transition back to subsonic flow has been neglected. For the subsonic flow solutions, the maximum of M^2 occurs at $y = (11 + M_{\rm max}{}^2)/10$, which lies between 1.1 and 1.2. Each solution is parametrized by the value of $M_{\rm max}$ or equivalently by the maximum value of σ which may in turn be derived from the value of the mass loss rate.

Finally we may investigate the conditions under which the evaporation is a steady-state process. If the cloud is in pressure equilibrium with its surroundings,

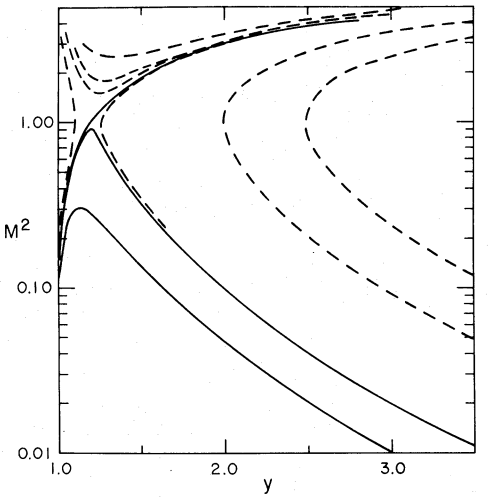

FIG. 1.—Possible solutions for the Mach number squared versus the normalized radius y ($=r/R$). For the transonic solution, the flow will ultimately undergo a weak shock beyond the sonic point and return to the subsonic curves.

the steady-state assumption will be valid provided the time $t_{\rm flow}$ for evaporating gas to flow from the surface of the cloud to a point at which $\tau \sim 1$ is small compared with $t_{\rm evap}$ defined in equation (22). We define $t_{\rm flow}$ to be the time required for the gas to reach $y = 1.5$, where $\tau = 0.64$. Since the Mach number is not large, the pressure is approximately constant throughout the flow and the flow time is given by

$$t_{\rm flow} = 1.70 \times 4\pi R^3 \rho_f / \dot{m} \qquad (28)$$

so that the condition for time independence is

$$\rho_c \gtrsim 5\rho_f \,. \qquad (29)$$

IV. SATURATED EVAPORATION

The solution for the evaporation rate derived in § III breaks down when the classical heat flux exceeds the saturated heat flux, i.e., $\sigma > 1$. From equations (9) and (19) we find that, in the classical solution,

$$\sigma = \left(\frac{2\kappa_f T_f}{25\phi_s \rho_f {c_f}^3 R}\right)\left(\frac{p_f \tau^{1/2}}{py^2}\right), \quad \sigma < 1 \,, \qquad (30)$$

which approaches zero at $y = 1$ and $y \to \infty$ and reaches a maximum in the interface. For sufficiently large T_f or sufficiently small $\rho_f R$ this maximum exceeds unity and the heat flux saturates.

It is convenient in discussing the evaporation to have a global rather than a local criterion for saturation. To this end, we collect the constants in the above expression for σ into the *saturation parameter* σ_0:

$$\sigma_0 = (2/25)\kappa_f T_f / \phi_s \rho_f {c_f}^3 R \,. \qquad (31)$$

Since the maximum value of $(p_f \tau^{1/2}/py^2)$ is of order unity, the condition for saturation [Max $(\sigma) > 1$] is equivalent to $\sigma_0 \gtrsim 1$; more precise values will be determined below. Using equation (5), we find that σ_0 is related to the mean free path λ_f in the ambient medium by $\sigma_0 = 1.84\lambda_f / R\phi_s$. Setting the Coulomb logarithm $\ln \Lambda = 30$ throughout, we find

$$\sigma_0 = \left(\frac{T}{1.54 \times 10^7 \text{ K}}\right)^2 \frac{1}{n_f R_{\rm pc} \phi_s} \,. \qquad (32)$$

What are the consequences of saturation of the conductivity in the interface on the evaporative mass loss rate? Because the incoming heat flux drops below the classical value, the evaporative mass loss rate tends to be less than the classical value of equation (21). However, there is a lower bound on $\dot{m}$: since the integrated heat flux must be $\gtrsim 5\phi_s \rho_f {c_f}^3 4\pi R^2$, we find $\dot{m} \gtrsim 8\pi R^2 \rho_f c_f \phi_s$. This crude minimum may substantially underestimate the evaporation from a spherical cloud, however, since the thickness of the zone between cloud and intercloud may be comparable to or even greater than R, thereby significantly increasing the integrated heat flux.

In this section we shall obtain an exact hydrodynamic solution for the evaporative mass loss rate in the case where the heat flux saturates in the interface. We shall assume that electron and ion temperatures are equal throughout the interface; this approximation will be discussed in § IV*f*.

a) Hydrodynamic Approximation

The principal approximation in our analysis is our use of the hydrodynamic equations of motion and energy conservation when the mean free path becomes large ($\lambda_f / R \gtrsim 1$). The exact time-independent equations of motion and energy conservation for a collisionless plasma are (e.g., Delcroix 1965)

$$\rho \boldsymbol{v} \cdot \nabla \boldsymbol{v} = -\nabla \cdot \boldsymbol{\Psi} \,, \qquad (33)$$

$$\nabla \cdot [\rho \boldsymbol{v}(\tfrac{1}{2}v^2 + u)] + \nabla \cdot (\boldsymbol{\Psi} \cdot \boldsymbol{v}) = -\nabla \cdot \boldsymbol{q} \,, \qquad (34)$$

where $\boldsymbol{\Psi}$ is the stress tensor and $u = (2\rho)^{-1} \operatorname{Tr} \boldsymbol{\Psi}$ is the internal energy per gram. We have assumed that plasma waves do not make a significant contribution to the momentum and energy balance of the plasma, although they may be important in maintaining the isotropy; hence we have neglected fluctuating currents and charge densities.

These equations reduce to the normal hydrodynamic equations provided only that the plasma is approximately isotropic and the stress tensor may be written as $\Psi_{ij} = p\delta_{ij}$. We shall assume subsequently that plasma instabilities maintain the required isotropy. We may note that in the case of the solar wind at 1 AU the anisotropy in pressure is less than 20% (Montgomery 1972*a*).

b) Structure of the Interface

The transition between the cloud and the ambient medium breaks up into three zones (Fig. 2): (1) the *inner classical zone*, extending from the cloud surface ($y = r/R = 1$) to a point y_{s1}, in which the heat flux is not saturated because the temperature and hence the classical conductivity are small; (2) the *saturated zone*

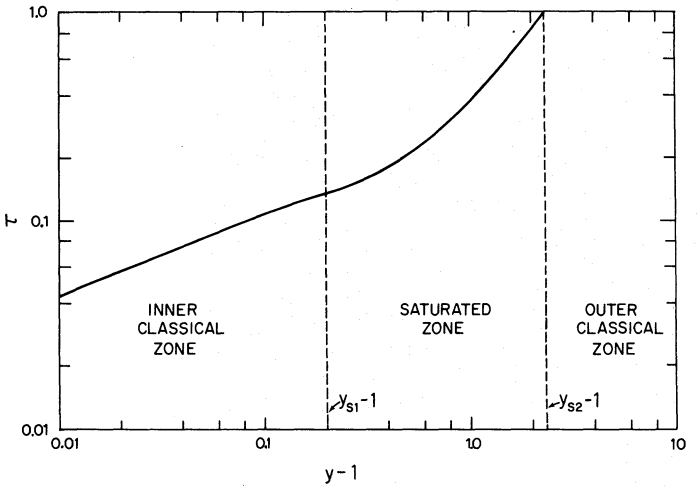

FIG. 2.—The temperature profile for the case of saturated evaporation with $\sigma_0 = 170$ and $M_s = 1$. The flow divides into three zones: $y < y_{s1}$ where the temperature is low and classical conduction is applicable, $y_{s1} < y < y_{s2}$ where the conduction is saturated, and $y > y_{s2}$ where the temperature gradient is small and the classical conduction is again applicable.

($y_{s1} < y < y_{s2}$) in which the heat flux is saturated; and (3) the *outer classical zone*, ($y > y_{s2}$), in which the heat flux is not saturated because the temperature gradient is small. Balancing the outward enthalpy flux and the inward heat flux at y_{s2} (i.e., integrating the energy eq. [12]) gives

$$\dot{m} = 4\pi R^2 \rho_f c_f [(2\phi_s/g)(p_{s2}/p_f)(c_f/c_{s2}) y_{s2}^2] . \quad (35)$$

All the factors in the brackets except y_{s2}^2, which reflects the increase in effective area mentioned above, are expected to be of order unity. We shall now proceed to demonstrate that this expression is physically self-consistent and to evaluate the factors in the brackets. In the interests of obtaining an analytic solution, the heat flux is taken to be either classical or saturated with abrupt transitions in functional form at y_{s1} and y_{s2}. Since temperature scale lengths and mean free paths vary rapidly in the interface, this should be an excellent approximation.

c) *Dynamics of the Saturated Zone*

In the case of classical evaporation it is possible to integrate the energy equation and obtain the temperature profile independently of the equations of motion. When the heat flux is saturated ($q_{\rm sat} = 5\phi_s \rho c^3$), this is no longer possible because q depends on ρ as well as on T. Integration of the energy equation does show that the Mach number M_s in the saturated zone is constant:

$$M_s(1 + \tfrac{1}{5}M_s^2) = 2\phi_s . \quad (36)$$

The relation between M_s and ϕ_s is shown in Figure 3. Since M_s is constant, the equation of motion can be easily integrated; in the notation of § III we find

$$\tau \propto y^{4/(1+M_s^2)} , \quad (37)$$

$$p \propto y^{-2M_s^2/(1+M_s^2)} , \quad (38)$$

$$\rho \propto y^{-2(2+M_s^2)/(1+M_s^2)} . \quad (39)$$

Note that such a steady-state solution would not be possible in the plane case since the equation of motion, has only the trivial solution of constant velocity, temperature, and density in this case.

The constant of proportionality in equation (37) may be found from equation (35). Defining the constant

$$\alpha = \sigma_0 (p_f/p_{s2}) y_{s2}^{-2M_s^2/(1+M_s^2)} , \quad (40)$$

after some straightforward algebraic manipulation we obtain

$$\tau = \{1/(\alpha w)^2\} y^{4/(1+M_s^2)} , \quad (41)$$

where w was defined in equation (15) as $\dot{m}/\dot{m}_{\rm class}$.

The Mach number M_s cannot be much greater than unity because ϕ_s is of order unity (eq. [36]). If the flow in the saturated zone is supersonic ($M_s \gtrsim 1$, or $\phi_s \gtrsim 0.6$), then a shock transition to subsonic flow must occur in the outer classical zone. Since this shock would be weak, it would have only a minor effect on the evaporation rate, and we shall ignore it.

d) *Solution for the Evaporation Rate*

The solutions just found for the temperature profile in the saturated zone must be matched to the solutions in the inner and outer classical zones in order to determine the three unknown quantities $w \propto \dot{m}$, y_{s1}, and y_{s2}.

The solutions for the classical zones may be obtained by the methods of § III. In the inner classical zone

$$\tau = w^{2/5}(1 - y^{-1})^{2/5} , \quad y \le y_{s1} ; \quad (42)$$

while in the outer classical zone

$$\tau = (1 - w/y)^{2/5} , \quad y \ge y_{s2} . \quad (43)$$

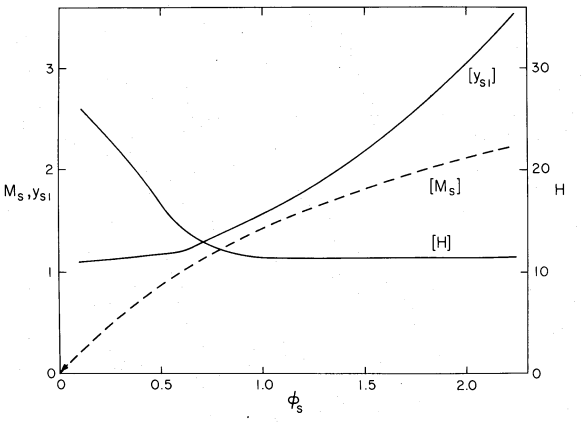

FIG. 3.—The Mach number of the saturated zone M_s, the position of its inner surface y_{s1}, and the constant H defined in eq. (52) are shown in terms of the factor ϕ_s defined in eq. (8).

Two equations are provided by matching these temperatures to those in the saturated zone at the zone boundaries,

$$y_{s1}{}^h/\alpha^5 w^6 - y_{s1} + 1 = 0\,, \tag{44}$$

$$y_{s2}{}^h/\alpha^5 w^6 - y_{s2}/w + 1 = 0\,, \tag{45}$$

where h is defined as

$$h \equiv (11 + M_s{}^2)/(1 + M_s{}^2)\,. \tag{46}$$

These equations also ensure continuity of the heat flux $q \propto \dot{m}c^2$. Note that α itself depends on both y_{s2} and p_{s2} (eq. [40]); the latter may be evaluated by integrating the equation of motion in the outer classical zone.

It is possible to complete the solution by finding an equation for y_{s1}. For supersonic flow ($M_s \geq 1$, $\phi_s \geq 0.6$) this is provided by the unique transonic solution of the equation of motion. The solution for $M(y)$ in the case of classical evaporation (see Fig. 1) remains valid in the inner classical zone in the case of saturated evaporation since $\tau(y)$ (eq. [42]) has the same functional form in the two cases. [Note that in the outer classical zone y must be replaced by y/w in order for $\tau(y)$ to have this form and for Fig. 1 to be applicable.] The value of y_{s1} is then determined by the point at which $M(y)$ reaches M_s (see Fig. 1).

For subsonic flow the situation is more complex since the flow in the inner classical zone is not unique. We shall show that $d\tau/dy$ and dM/dy are continuous at y_{s1} and that this allows y_{s1} to be determined. Note that the continuity of $d\tau/dy$ at y_{s1} does not follow from the continuity of the heat flux q since in the saturated zone q is independent of the temperature gradient. The equation of motion may be written in the form

$$\frac{d\ln M^2}{dy} = \frac{(1 + M^2)}{(1 - M^2)}\frac{d\ln\tau}{dy} - \frac{4}{(1 - M^2)y}\,, \tag{47}$$

which is applicable in all three zones. It follows that for subsonic flow any discontinuity in $d\tau/dy$ at y_{s1} will be accompanied by a discontinuity in dM/dy of the same sign. Now $d\tau/dy \propto \sigma$, the ratio of the classical to the saturated heat flux; $\sigma \to 1$ as $y \to y_{s1}$ from below and σ cannot decrease at y_{s1} if the heat flux is to be saturated for $y \gtrsim y_{s1}$. Hence any discontinuity in $d\tau/dy$ at y_{s1} must be nonnegative. On the other hand, in the inner classical zone $\sigma = Mg/2\phi_s$ (eq. [23]) and $dM/dy \propto d\tau/dy > 0$ up to the point of saturation. Since $M = M_s$ = constant in the saturated zone, dM/dy can only undergo a nonpositive discontinuity at y_{s1}. These two results are consistent only if $d\tau/dy$ and dM/dy are both continuous at y_{s1}; in particular $dM/dy = 0$ at y_{s1}.

(Note that a similar argument cannot be used to show that $d\tau/dy$ and dM/dy are continuous at y_{s2}, the outer boundary of the saturated zone, since both quantities have the same sign there and eq. [47] is not violated.)

We can now determine y_{s1} for subsonic flow: it is the point at which $dM/dy = 0$, so that M is a maximum. In § III*b* it was shown that M attains its maximum value at $y = (11 + M_{\max}{}^2)/10$ so that

$$y_{s1} = (11 + M_s{}^2)/10 = h/(h - 1)\,, \tag{48}$$

where h is given by equation (46).

Having found y_{s1} for both the subsonic and supersonic cases, we can solve equation (44) for the normalized mass loss rate

$$w = H^{1/6}\alpha^{-5/6}\,, \tag{49}$$

where

$$H = y_{s1}{}^h/(y_{s1} - 1)\,. \tag{50}$$

Both y_{s1} and H are plotted as functions of M_s in Figure 3. In the subsonic case y_{s1} is given by equation (48) and

$$H = h^h/(h - 1)^{h-1} \quad (M_s \leq 1)\,. \tag{51}$$

In the supersonic case H is approximately constant and equal to 11.5.

Equation (49) for w depends on y_{s2} and p_{s2} through α and must be solved together with equation (45). Before developing an approximate solution for these equations, we note that in general

$$w \leq 1\,, \tag{52}$$

so that the effect of saturation is to reduce the evaporation rate below the classical value. This can be demonstrated by combining equations (44) and (45) to give

$$w = \frac{(y_{s2}/y_{s1})y_{s1}}{1 + (y_{s1} - 1)(y_{s2}/y_{s1})^h} \tag{53}$$

and applying the inequalities $y_{s2}/y_{s1} \geq 1$, $h > 1$, and $y_{s1} \geq h/(h - 1)$ (in this last condition, equality corresponds to $M_s \leq 1$; the inequality for $M_s > 1$ follows from the condition $\sigma \leq 1$ for $y \lesssim y_{s1}$).

The transition from classical to saturated evaporation occurs at $w = 1$ and $y_{s1} = y_{s2}$. The value of σ_0 at the onset of saturation can then be found from equations (40) and (49),

$$\sigma_0(\text{onset}) = (p_{s2}/p_f) y_{s1}^{11/5}/(y_{s1} - 1)^{1/5} . \quad (54)$$

Using the approximation for p_{s2}/p_f given in equation (56) below, one finds that σ_0(onset) is of order unity, as expected: for $M_s \approx 2\phi_s \ll 1$, σ_0(onset) = 1.95; for $M_s^2 = 2$ and $\phi_s = 1$, σ_0(onset) = 1.08.

e) *Highly Saturated Evaporation*

While equations (45) and (49) may always be solved numerically in order to obtain the evaporation rate, it is possible to find an analytic solution for the highly saturated case ($\sigma_0 \gg 1$) which turns out to also provide a good approximation for the nearly classical case ($\sigma_0 \sim 1$).

In the highly saturated case, one has $\alpha \sim \sigma_0 \gg 1$ and $w \sim \alpha^{-5/6} \ll 1$ so that the temperature in the outer classical zone (eq. [43]) is very nearly constant. Combining equations (26) and (47) for the case of isothermal flow yields

$$\frac{d \ln p}{dr} = -\frac{1}{2} \frac{dM^2}{dr} , \quad (55)$$

which may be integrated to give the pressure at y_{s2},

$$p_{s2} = p_f \exp(-\tfrac{1}{2} M_s^2) . \quad (56)$$

Since we have ignored the weak shock which is present in the outer classical zone in the case of supersonic flow, this result is strictly valid only for $M_s^2 < 1$. However, we shall adopt it as an approximation for all cases.

The solution for y_{s2} and w may now be obtained. Using equation (49) and applying the conditions $\alpha \gg 1$ and $w \ll 1$, we can approximate equation (45) as

$$y_{s2}^{h-1} = (\alpha H)^{5/6} . \quad (57)$$

Solving this equation simultaneously with equation (40) for α gives

$$y_{s2} = [\sigma_0 H \exp(\tfrac{1}{2} M_s^2)]^{0.5(1+M_s^2)/(6+M_s^2)} , \quad (58)$$

which is a weakly varying function of σ_0. Substitution of this result into equation (49) then leads to an explicit form for w:

$$w = [\sigma_0^{-5} H^{1+M_s^2} \exp(-2.5 M_s^2)]^{1/(6+M_s^2)} . \quad (59)$$

Although these results have been derived from the assumption $w \ll 1$, they provide a good approximation even at the onset of saturation when $w = 1$, agreeing with numerical calculations to within 30%. Expression (56) for p_f/p_{s2} is within 6% of numerical calculations for the case of classical evaporation with $\phi_s = 0.6$ and a maximum Mach number of 0.99, which corresponds to the onset of saturation.

In view of the fact that our results for highly saturated evaporation provide a good approximation for all cases of saturated evaporation, a more convenient form for the mass loss rate $\dot{m}$ is called for. In general, define the function $F(\sigma_0)$ by

$$\dot{m} = 4\pi R^2 \rho_f c_f \phi_s F(\sigma_0) . \quad (60)$$

In the classical case one finds

$$F(\sigma_0) = 2\sigma_0 , \quad (61)$$

whereas in the saturated case

$$F(\sigma_0) = 2[(\sigma_0 H)^{1+M_s^2} \exp(-2.5 M_s^2)]^{1/(6+M_s^2)} . \quad (62)$$

As is shown in Figure 4, F is of order unity for σ_0 of order unity; furthermore, F depends only weakly on M_s or ϕ_s. Numerically, the saturated mass loss rate is

$$\dot{m} = 3.25 \times 10^{18} n_f T_f^{1/2} R_{pc}^2 \phi_s F(\sigma_0) \text{ g s}^{-1} , \quad (63)$$

where for $\phi_s = 1$, for example, $F(\sigma_0) = 2.73\sigma_0^{3/8}$. The corresponding evaporation time is

$$t_{\text{evap}} = 2.8 \times 10^6 (\bar{n}_c/n_f) R_{pc}/[T_f^{1/2} \phi_s F(\sigma_0)] \text{ yr} . \quad (64)$$

The dependence of $\dot{m}$ on the basic variables n_f, T_f, and R is

$$\dot{m} \propto [n_f^5 T_f^{2.5(2+M_s^2)} R^{11+M_s^2}]^{1/(6+M_s^2)} . \quad (65)$$

The variation of temperature with radius is shown for the particular case $\sigma_0 = 170$ and $M_s = 1$ in Figure 2. The saturated zone extends from $1.2R$ to $2.3R$. As discussed in § IV*d*, the temperature gradient is continuous at y_{s1} and discontinuous at y_{s2}; the latter is an artifact of the abrupt switch in the functional form of the conductivity at the zone boundaries.

Finally we may note that for highly saturated evaporation the pressure in the cloud may substantially exceed the ambient pressure. Numerical integration shows that the pressure drop in the inner

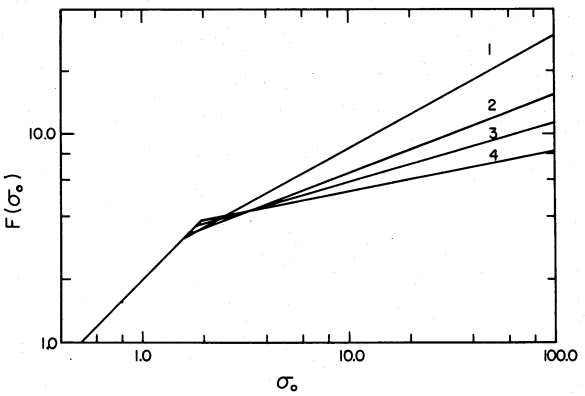

FIG. 4.—The function $F(\sigma_0)$ defined in eqs. (61) and (62) plotted as a function of σ_0. The break in the profile corresponds to the onset of saturation. (1) $M_s^2 = 5$, $\phi_s = 2.24$. (2) $M_s^2 = 2$, $\phi_s = 1$. (3) $M_s^2 = 1$, $\phi_s = 0.60$. (4) $M_s^2 = 0.2$, $\phi_s = 0.23$.

classical zone is $p_{s1}/p_c \approx \exp(-0.8M_s^2)$. Combining this with the above results gives

$$\frac{p_c}{p_f} = [\sigma_0 H \exp(1.8 + 0.8M_s^2)]^{M_s^2/(6+M_s^2)} y_{s1}^{-2M_s^2/(1+M_s^2)}, \quad (66)$$

so that for $\phi_s = 1$ one has $p_c/p_f = 2.43\sigma_0^{1/4}$.

f) Limitations

We now analyze the limitations imposed on our results by our assumptions. In addition to explicitly assuming that the evaporation is a steady-state process and that the electron and ion temperatures are equal, we have also implicitly assumed that the electron mean free path is not too long, as we now discuss.

1. *Mean free path approximation.*—The saturated zone in effect forms an insulating region between the hot ambient gas and the cool cloud. At the outer boundary of the saturated zone, the mean free path of the electrons can greatly exceed the temperature scale height. However, we require that the range of the hot electrons be less than the thickness of the saturated zone. Otherwise, the hot electrons could penetrate into the inner classical zone, where we have explicitly assumed that the mean free path is small. An additional effect which occurs at this point is that heat flux may no longer be carried by the electrons which determine the temperature (§ II); however, the value of the saturated heat flux does not depend critically on this assumption.

What is the condition placed on the saturation parameter σ_0 by the condition that the ambient electrons be unable to penetrate the saturated zone? In highly saturated flow, the hot electrons are suprathermal in much of the saturated zone, and they can penetrate a column density $n_f\lambda_f/8$ (see Spitzer 1962), where λ_f is the thermal mean free path defined in § II. The column density of the saturated zone in this case is

$$N_{\rm sat} = n_f R\left(\frac{1+M_s^2}{3+M_s^2}\right)[(\sigma_0 H)^{2+M_s^2}\exp(-2M_s^2)]^{1/(6+M_s^2)} \times y_{s1}^{-(3+M_s^2)/(1+M_s^2)}, \quad (67)$$

which amounts to $0.61\sigma_0^{1/2}n_f R$ at $\phi_s = 1$. Comparing this with $n_f\lambda_f/8$, we find that our approximation breaks down at $\sigma_0 \approx 100\phi_s^{-1}$. Even above this value of σ_0, however, we expect that our results should remain qualitatively correct until ultimately the range $n_f\lambda_f/8$ approaches the cloud column density $\bar{n}_c R$ and the theory breaks down completely; this occurs at $\sigma_0 \approx 15\bar{n}_c/n_f\phi_s$.

2. *Steady state.*—As discussed in § III, the assumption that the evaporation is a steady-state process is justified if the evaporation time $t_{\rm evap}$ is much greater than the time $t_{\rm flow}$ for the evaporating gas to flow from the cloud to a point at which $\tau \sim 1$. For $\sigma_0 \lesssim 10^3\phi_s^{-1}$ we find

$$t_{\rm flow} \approx Ry_{s2}/(M_s c_f). \quad (68)$$

This must be less than $t_{\rm evap}$ given in equation (64), which leads to the condition

$$\bar{n}_c/n_f > 3(\sigma_0 H)^{1.5(1+M_s^2)/(6+M_s^2)}. \quad (69)$$

For example, for $\phi_s = 1$ this becomes $\bar{n}_c/n_f \gtrsim 12\sigma_0^{0.56}$.

3. *Ion-electron equipartition.*—For simplicity we have set $T_i = T_e$ in our analysis. The ion temperature is controlled by electron-ion collisions except in the outer parts of the saturated zone, where ion-ion collisions may dominate. Comparison of the electron-ion heating rate with the term $kvdT/dr$ shows that $T_e \sim T_i$ in most of the inner classical zone, but T_i rapidly drops below T_e within the saturated zone. The main effect of this is to enhance the efficiency of the evaporation process since the electron temperature remains higher than it would otherwise be. This may be approximately included by multiplying ϕ_s by a factor of $2^{3/2}$ (see § II); as can be seen from equation (60), this leads to a comparable increase in the evaporation rate.

V. CONDUCTION FRONTS

McKee and Cowie (1975) have analyzed the evaporation process in terms of a conduction front advancing into the cooler gas. This analysis is based on the one-dimensional equations of mass and momentum conservation; the energy conservation equation is not considered. Just as in the case of ionization fronts (e.g., Spitzer 1968), the velocity of the front $v_{\rm cond}$ relative to the gas ahead of the front must be less than $\frac{1}{2}c_c^2/c_f$ (D-type front; rarefaction) or greater than $2c_f$ (R-type front; compression). Furthermore, the fronts can be characterized as "weak" or "strong" depending on the magnitude of the density jump across the front; in particular, a weak R-type front has a small density jump and moves supersonically relative to both the gas ahead of the front and the gas behind the front. We have previously argued that plasma instabilities prevent the occurrence of weak R-type conduction fronts.

Here we have improved upon our previous treatment by integrating the energy equation and including the effects of spherical divergence. This allows a determination of the velocity of the conduction front

$$v_{\rm cond} = \dot{m}/4\pi R^2\rho_c. \quad (70)$$

For classical evaporation, equations (60) and (61) give

$$v_{\rm cond} = 2\sigma_0\phi_s(p_f/p_c)(c_c^2/c_f). \quad (71)$$

Since in this case $\sigma_0 \lesssim 1$ and in general $p_f/p_c \lesssim 1$, we find $v_{\rm cond} \lesssim c_c^2/c_f$. Hence classical conduction fronts are D-type, as suggested by McKee and Cowie (1975).

For saturated evaporation, equations (62) and (65) give

$$v_{\rm cond} = 2\phi_s\{\sigma_0 H \exp\,[-M_s^2(4.3 + 0.8M_s^2)]\}^{1/(G+M_s^2)} \times y_{s1}^{2M_s^2/(1+M_s^2)}\left(\frac{c_c^2}{c_f}\right), \quad (72)$$

which leads to $v_{\rm cond} = 1.12\sigma_0^{1/8}c_c^2/c_f$ for $\phi_s = 1$. Since the coefficient of c_c^2/c_f is of order unity in equation (72), we conclude that saturated conduction fronts are approximately D-critical. The fact that both the classical and the saturated conduction fronts are D-type is a consequence of our assumption that the cloud density is much greater than the ambient density (see §§ III*b* and IV*f*). If the front were to be an R-type front, a region of extremely high pressure would occur near the cloud because the density as well as the temperature increases behind such a front. This high-pressure layer would rapidly expand and relax to the pressure distribution appropriate for a D-type front.

Even if we drop the assumption that the hot gas has a much lower density than the cold gas, the saturation of the heat flux limits the nature of the front. For one-dimensional R-type fronts with negligible radiative losses, one can show that the velocity of the front cannot greatly exceed $2c_f$:

$$\frac{v_{\rm cond}}{2c_f} = \frac{5\phi_s^2 + 0.8}{\phi_s + 2(\phi_s^2 + 0.12)^{1/2}}. \quad (73)$$

For $\phi_s = 1$, one finds $v_{\rm cond} = 1.86(2c_f)$. Hence, in a uniform medium, weak R-type conduction fronts are limited to relatively low velocities by the saturation of the heat flux; by contrast, weak R-type ionization fronts can propagate at up to the speed of light. For $\phi_s \sim 1$ there is no limitation on strong R-type fronts. If $\phi_s < 0.2$, however, $v_{\rm cond}$ is less than $2c_f$ and no R-type front is possible.

Similar considerations apply to problems other than evaporation: a particularly interesting example is the case of a strong point explosion (e.g., a supernova remnant). In the early stages of the evolution of such a system, the temperature is too high for the classical conduction formula to be applicable, and the conduction is saturated. Incorrect use of the classical conduction formula in this phase of the evolution then results in a weak R-type front which propagates much faster than the blast-wave shock (Chevalier 1975*a*). When the saturated heat flux is used, the velocity of conduction front is constrained to be close to that of the blast-wave shock, and plasma instabilities will probably make the front and the shock coincident. In that case the volume of the heated gas is approximately the same as in the normal blast-wave solution (e.g., Woltjer 1972).

VI. EVAPORATION OF CLOUDS WITHIN SUPERNOVA REMNANTS

We have assumed in deriving the results of §§ III and IV that the temperature distribution of the hot gas is isotropic and that dynamical effects may be neglected. As such, the results are not directly applicable to certain systems of interest, in particular the evaporation of clouds which have been overtaken by a shock wave. In this case, the cloud may no longer be in pressure equilibrium with its surroundings, and convective energy transfer and the presence of bow shocks may result in temperature anisotropy and in perturbations of the temperature gradients.

McKee and Cowie (1975) have extensively discussed the dynamical interaction of an initially stationary cloud with a supernova blast wave, while Sgro (1975) has given numerical simulations of this problem. After the cloud has been engulfed by the blast wave, it is penetrated by a shock wave driven by the ram and thermal pressures of the surrounding material. Initially a bow shock forms in the surrounding material, which eventually disappears when the flow of the surrounding material relative to the cloud becomes subsonic. McKee and Cowie (1975) have demonstrated that the time for a shock to cross the cloud is short compared with the evaporation time scale; on the other hand, the shock crossing time is generally much greater than $t_{\rm flow}$, the time for the evaporating gas to flow across the conductive interface. Hence, we may neglect the internal dynamics of the cloud in evaluating the evaporation rate, and treat the cloud as instantaneously stationary.

Similar arguments may also be applied to the evaporation of a cloud or knot moving supersonically in a stationary cool gas (Chevalier 1975*b*). In this case the bow shock can be strong.

The flow of the hot ambient gas around the cloud has several effects. First, it tends to bend the magnetic field in the evaporating gas back around the cloud, which reduces the evaporation rate. This effect is less important if the evaporative flow velocity exceeds the velocity of the flow past the cloud, but the magnitude of the effect is difficult to estimate. Second, the flow may lead to turbulent mixing of the cool cloud with the hot gas, which both increases the effective surface area for evaporation and tangles the magnetic field.

A third effect is that convective energy transport can increase the temperature gradient and hence, in the classical case, increase the evaporation rate. If the flow velocity around the cloud is related to the local sound speed by the equation $v \equiv \delta c$ ($\delta < 1$), comparison of convective ($1.5\rho c^2 v$) and conductive energy transfer ($\kappa T/L$, where L is the temperature scale length) indicates that convective energy transfer can maintain the temperature at $T \sim T_f$ for radii $y \gtrsim 1 + (\sigma_0/\delta)^{1/2}$. (In deriving this result, we have assumed that the scale lengths are small compared with the cloud radii, $\sigma_0/\delta \ll 1$.) The resulting classical rate, based on arguments similar to those of § III, is of order

$$\dot{m}_{\rm class.anis.} = \dot{m}_{\rm class}(\sigma_0/\delta)^{-1/2}, \qquad (\sigma_0/\delta)^{1/2} \ll 1. \quad (74)$$

If, on the other hand $\delta \lesssim \sigma_0$, the usual classical evaporation rate is applicable, and the relative flow may be ignored. In terms of the general mass loss

equation, (60), equation (74) corresponds to $F(\sigma_0) = 2(\sigma_0\delta)^{1/2}$ which decreases less rapidly with σ_0 than the isotropic rate $F(\sigma_0) = 2\sigma_0$. The enhancement of the evaporation rate over the isotropic value is limited to a factor of about 5 since, as shown in Paper II, radiative losses quench the evaporation for $\sigma_0 \lesssim 0.03\phi_s$.

For the case of saturated evaporation, convective energy transport has a small effect since the flow behind the shock is subsonic, whereas the evaporative flow occurs at about the sound speed. Because of the evaporation the exact position of the bow shock is uncertain. For a nonevaporating spherical cloud, $y_{\rm shock} = 1.2$ in the highly supersonic case (e.g., Hayes and Probstein 1963); for the more general case this value is a lower bound. If the bow shock occurs close to the cloud, the saturated evaporation from the front of the cloud may be somewhat reduced, although in the absence of a magnetic field it must always exceed $4\pi R^2\rho_f c_f$, where ρ_f and c_f are now average values of ρ and c just behind the bow shock. Note that this minimum corresponds to setting $\phi_s F = 1$ in the expressions for $\dot{m}$ (eqs. [60] and [63]) and probably provides a reasonable estimate for $\dot{m}$ in this case.

VII. SUMMARY

We have derived expressions for the rate of evaporative mass loss in a hot medium under the assumption that both radiative and magnetic effects can be neglected. In terms of the saturation parameter σ_0 (eq. [32]), which is proportional to the ratio of the mean free path to the cloud radius, the results split into two cases. For $\sigma_0 \lesssim 1$, the classical thermal conductivity is applicable and the mass loss rate $\dot{m}$ is given by equation (21) in § III. The flow is generally subsonic in this case and the pressure in the cloud is only somewhat greater than that in the ambient medium. For $\sigma_0 \gtrsim 1$, the thermal conduction in the outer part of the conductive interface saturates at a value $5\phi_s\rho c^3$, where ϕ_s is an unknown constant which theoretical and observational arguments suggest is of order unity (§ II). The mass loss rate is now given by equation (63). The flow in the saturated zone occurs at a constant Mach number, M_s, which is related to ϕ_s by equation (36) (see Fig. 3). For saturated evaporation, the pressure in the cloud can significantly exceed that in the ambient medium. Analysis of the limitations of our theory in § IV*f* shows that it is accurate only for $\sigma_0 \lesssim 100/\phi_s$, although it should provide a reasonable approximation at even higher values of σ_0.

Applications of these results will be deferred to Paper II. There we shall demonstrate that radiative losses can stop evaporation for $\sigma_0 \lesssim 0.03/\phi_s$, so that the domain of classical evaporation ($0.03/\phi_s \lesssim \sigma_0 \lesssim 1$) is comparable to the domain of saturated evaporation which is accurately treated by our theory ($1 \lesssim \sigma_0 \lesssim 100/\phi_s$). In Paper III we shall show that under a wide variety of conditions the presence of a magnetic field in the evaporating gas does not significantly inhibit the evaporation.

We thank G. Field, C. Max, J. Arons, and B. Elmegreen for helpful comments. This research was supported in part by NSF grant AST 75-02181. L. L. C. gratefully acknowledges the support and hospitality of the Center for Astrophysics during the course of this work.

REFERENCES

Castor, J., McCray, R., and Weaver, R. 1975, *Ap. J. (Letters)*, **200**, L107.
Chevalier, R. A. 1975*a*, *Ap. J.*, **198**, 355.
———. 1975*b*, *Ap. J.*, **200**, 698.
Cox, D. P., and Smith, B. W. 1974, *Ap. J. (Letters)*, **189**, L105.
Cuperman, S., and Metzler, N. 1973, *Ap. J.*, **182**, 961.
Delcroix, J. L. 1965, *Plasma Physics* (London and New York: Wiley).
De Young, D. S. 1973, preprint.
Feldman, W. C., Asbridge, J. R., Bame, S. J., and Montgomery, M. D. 1973, *J. Geophys. Res.*, **72**, 3697.
Field, G. B. 1965, *Ap. J.*, **142**, 531.
Forslund, D. W. 1970, *J. Geophys. Res.*, **75**, 17.
Graham, R., and Langer, W. D. 1973, *Ap. J.*, **179**, 469.
Hayes, W. D., and Probstein, R. F. 1959, *Hypersonic Flow Theory* (New York: Academic Press).
Hollweg, J. V. 1974, *J. Geophys. Res.*, **79**, 3845.
Jenkins, E. B., and Meloy, D. A. 1974, *Ap. J. (Letters)*, **193**, L121.
Lea, S. M. 1974, Ph.D. thesis, University of California, Berkeley.
Manheimer, W. M., and Klein, H. H. 1975, *Phys. Fluids*, **18**, 1299.
McKee, C. F., and Cowie, L. L. 1975, *Ap. J.*, **195**, 715.
———. 1977*a*, submitted to *Ap. J.* (Paper II).
———. 1977*b*, in preparation (Paper III).
McKee, C. F., and Ostriker, J. P. 1975, *Bull. AAS*, **7**, 419.
Montgomery, M. D. 1972*a*, *J. Geophys. Res.*, **77**, 5503.
———. 1972*b*, *J. Geophys. Res.*, **77**, 5432.
Morse, R. L., and Nielsen, C. W. 1973, *Phys. Fluids*, **16**, 909.
Parker, E. N. 1963, *Interplanetary Dynamical Processes* (New York: Interscience).
Penston, M. V., and Brown, F. E. 1970, *M.N.R.A.S.*, **150**, 373.
Perkins, F. 1973, *Ap. J.*, **179**, 637.
Sgro, A. G. 1975, *Ap. J.*, **197**, 621.
Solinger, A., Rappaport, S., and Buff, J. 1975, *Ap. J.*, **201**, 381.
Spitzer, L. 1956, *Ap. J.*, **124**, 20.
———. 1962, *Physics of Fully Ionized Gases* (New York: Interscience).
———. 1968, *Diffuse Matter in Space* (New York: Interscience).
Weibel, E. S. 1959, *Phys. Rev. Letters*, **2**, 83.
Williams, M. M. R. 1971, *Mathematical Methods in Particle Transport Theory* (New York: Wiley-Interscience).
Williamson, F. O., Sanders, W. T., Kraushaar, W. L., McCammon, D., Borken, R., and Bunner, A. N. 1974, *Ap. J. (Letters)*, **193**, L133.
Woltjer, L. 1972, *Ann. Rev. Astr. Ap.*, **10**, 129.
Zel'dovich, Ya. B., and Pikel'ner, S. B. 1969, *J. Eksp. Teoret. Phys.*, **29**, 170.
Zel'dovich, Ya. B., and Raizer, Yu. P. 1966, *Physics of Shock Waves and High Temperature Hydrodynamic Phenomena* (New York: Academic Press).

LENNOX L. COWIE: Princeton University Observatory, Peyton Hall, Princeton, NJ 08540
CHRISTOPHER F. MCKEE: Physics Department, University of California, Berkeley, CA 94720